DOI: 10.61782/fa.2023.0417

IDENTIFICATION OF MICROSTRUCTURAL DESCRIPTORS CHARACTERIZING THE MACRO-BEHAVIOR OF HETEROGENEOUS RANDOM FIBROUS MEDIA

Quang Vu Tran[1,2,3*] **Camille Perrot**[1] **Raymond Panneton**[3]
Minh Tan Hoang[2] **Ludovic Dejaeger**[2] **Valerie Marcel**[2]
[1] Univ Gustave Eiffel, Univ Paris Est Creteil, CNRS, UMR 8208, MSME, F-77454 Marne-la-Vallée, France
[2] Adler Pelzer Group, Acoustic TechCenter R&D, Z.I. François Sommer – BP13, 08210 Mouzon, France
[3] Département de Génie Mécanique, Université de Sherbrooke, Québec J1K 2R1, Canada

ABSTRACT

This work is concerned with the multiscale prediction of the transport properties associated with thermo-compressed materials as recycled cotton felts bonded with petro-sourced fibers (Co-PET/PET). First, a geometric characterization is performed on the studied sample using scanning electron microscopy to identify the main microstructural descriptors (fiber angular orientation, fiber diameter polydiversity). Second, two representative volume elements (RVEs) of the sample are built: one for estimating the low-frequency transport parameters and one for estimating the the high-frequency transport parameters. Each RVE is built with rectilinear fibers parameterized by the probability density function of the fiber orientation and an appropriate weighted diameter. For the low-frequency RVE, a volume-weighted mean diameter is used, and an inverse volume-weighted mean diameter is used for the high-frequency RVE. These two RVEs make it possible to estimate the transport parameters in low and high frequency asymptotic behaviors using numerical homogenization methods. Finally, the estimated transport parameters are successfully compared to experimental measurements. The results demonstrate the role of the diameter polydispersity on the transport properties of random fibrous structures.

Keywords: *Multi scale simulations, microstructure, micro-macro, random fibrous media, polydisperse, heterogeneous, representative volume elements*

1. INTRODUCTION

Textile materials like thermo-compressed felts are widely utilized, particularly due to their sound insulation and absorption properties. The primary objective of this study is to establish robust models for predicting the acoustic behavior of fibrous media of industrial interest. These materials are characterized by local heterogeneities due to the increased presence of polydisperse fibers from recycled textiles and a manufacturing process involving thermo-compression (composite material). To achieve this objective, it is essential to develop a multi-scale methodology in order to link the local geometry and the acoustic macro-behavior to guide manufacturing and optimize the acoustic performance. Several studies proposed analytical expressions to determine the transport properties of fibrous materials [1–5]. While Refs. [1–3] focused on the prediction of the low frequency viscous transport parameters (resistivity σ or viscous permeability k_0), Refs. [4, 5] also addressed the determination of the remaining low-frequency (thermal permeability k_0') and high-frequency (tortuosity α_∞ together, thermal Λ' and viscous Λ characteristic lengths) parameters. By using microstructural approach, Luu et al. [6–8] developed a model for analyzing the acoustic behavior of uncompressed fibrous media composed of monodiperse Asclepias fibers. Additionally, He et al. [9] worked out a model for predicting transport properties with application to industrial glass wool, char-

---

***Corresponding author**: *quang-vu.tran@u-pem.fr.*

acterized by strongly polydisperse fibers (both in diameter and length). When using these models on polydisperse fibrous materials, the agreement between the transport parameters measured and those predicted using microstructural data as inputs, may still lack precision.

Here, the frequency-dependent response function of a rigid porous medium saturated by a visco-thermal fluid is considered. At low-frequencies, the porous medium is characterized by a isothermal viscous behavior. At high-frequencies, the porous medium is charasterized by an adiabatic inertial behavior. The authors believe that the low-frequency transport parameters are essentially governed by the largest pore sizes, while the high-frequency transport parameters strongly depend on the regions of the porous structure where the specific surface area is the highest. This may explain the lack of precision of existing models which do not make this distinction in the calculation of the transport parameters. To overcome the lack of accuracy of the existing models, a model that employs two different representative volume elements (RVEs) with distinct microstructural descriptors is proposed: one for the low-frequency parameters, and one for the high-frequency parameters. In this work, the construction of each RVE involves two distinct sets of fiber microstructural descriptors. At low frequencies, the volume weighted mean diameter (D_v) is used, while at high frequencies, the inverse-volume-weighted mean diameter (D_{iv}) is proposed.

The paper is structured as follows. Sec.2 reports characterizations at both micro- and macro- scales. Sec.3 presents the construction of the two RVEs and solves the corresponding boundary value problems from which the transport parameters of interest are determined. Sec.4 compares the numerical results with measurements.

2. MATERIALS AND EXPERIMENTAL APPROACH

In this work, cotton felts made up from cotton fibers bounded with petro-sourced fibers are considered.

2.1 Microstructure characterization

The microstructure of the felt is characterized using (SEM) images acquired on two horizontal planes and two vertical planes of a cubic sample. The morphology parameters of the fibrous network are obtained using FiJi software [10]. These parameters include the diameter of the fibers and their orientation angles in the horizontal and vertical planes, as shown in Fig. 1. Using a non-parametric kernel method, the probability density functions of fiber diameter, the azimuthal and zenithal angles are shown in Fig. 2. Fig.1b reveals a probability density function characterizing polydisperse fiber diameters (non symmetric with a relatively long tail). The dominant mode displayed a majority of fibers with a diameter of 11 μm. Moreover, the right hand side of the distribution also indicates a relative small number of very large fibers. The azimuthal angle φ is distributed uniformly between 0^o and 180^o. The zenithalal angle θ^o is characterized by a mean orientation angle $\mu_\theta = 91.9^o$ (close to 90^o) and a standard deviation $\sigma_\theta = 36.2^o$ (large dispersion of the angular orientation of fibers).

2.2 Experimental characterization of transport and acoustic properties

The open porosity is determined using the pressure/mass method, which involves measuring four masses at four static pressures and applying the perfect gas law [11]. The static airflow resistivity σ is measured in a laminar regime using the standard method ISO 9053-1:2018. The tortuosity α_∞ is measured using the ultrasound transmission technique at high frequencies, as described in [12].

The Kozeny-Carman formula approach is used in [13] to determine the two characteristic lengths Λ and Λ'. This approach involves using the directly measured values for the porosity ϕ, the resistivity σ, and the tortuosity α_∞. Although direct measurements for viscous characteristic length Λ and thermal characteristic length Λ' were not possible, it seems that the Kozeny-Carman formula does not invalidate the simulated values. On the contrary, the order of magnitude and the proximity of the simulated values to the calculated values allow us to conclude that the simulated values are reliable (2, Two-RVE). The static thermal permeability k'_0 is determined by [14] using the low-frequency Champoux-Allard description of the thermal characteristic length Λ'_{lf}.

3. MULTI-SCALE RECONSTRUCTION TECHNIQUE

Considering the challenge of accurately predicting the acoustic properties of highly-dispersed fiber media using current models, we suggest the use of novel 3D network models that incorporate two weighted diameter parameters, as well as fiber orientation and porosity, to address this issue.

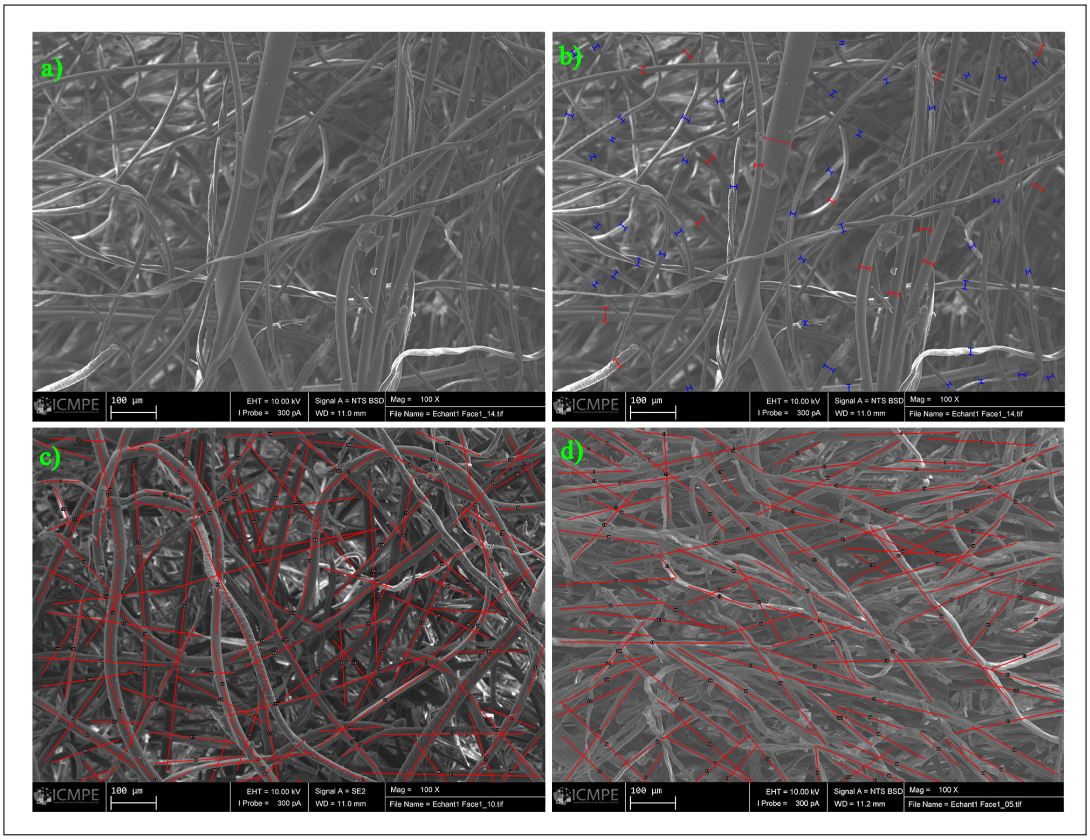

Figure 1: Scanning electron microscope (SEM) and measurements with Fiji software for the cotton felt; (a) top view of cotton felt sample; measurements of (b) fiber diameter; (c) azimuth angle; and (d) zenith angle.

3.1 Reconstruction of two distinct Representative Volume Elements

The anisotropy parameter β, characterizing the orientation distribution using polar coordinates Fig. 2a, can be written as the probability density function $p_\beta(\theta,\varphi)$ [15]:

$$p_\beta(\theta,\varphi) = \frac{1}{4\pi}\frac{\beta\sin\theta}{(1+(\beta^2-1)\cos^2\theta)^{3/2}}. \tag{1}$$

For the determination of the β value, two criteria are used. The first criterion consists in minimizing the difference between the modeled and the experimental probability density functions of the zenithal angle θ. The second criterion corresponds to the minimization of the difference between the standard deviation θ^o of the model and the experimental data, by selecting the most suitable anisotropy parameter β (see Fig. 2c and Fig. 2d). In practice, both criteria coincide.

The Gamma distribution was found to be in good agreement with the experimental results to model the fiber diameter distribution (Fig. 2b). The coefficient of variation (CV) used as a parameter representative of the polydispersity is computed as the ratio of the standard deviation to the mean $(CV = \sigma_D/\mu_D)$ (see Fig. 2b).

Two weighted mean diameters are proposed for the fiber polydisperse medium:

The volume-weighted mean diameter D_v [9, 16] is calculated by assigning each fiber a weight proportional to its diameter, weighted by its relative volume in the calculation of the arithmetic mean. It is given by

$$D_v = \frac{1}{\sum_{i=1}^{N_f} V_i}\sum_{i=1}^{N_f} V_i D_i. \tag{2}$$

where V_i and D_i are the volume and diameter associated with the i^{th} fiber, and N_f is the number of fibers.

The inverse volume-weighted mean diameter D_{iv} is computed by assigning each fiber a weight proportional to its

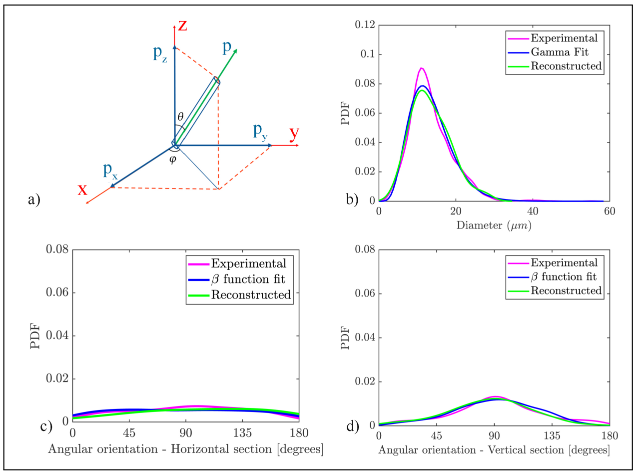

Figure 2: (a) The orientation of a fiber in three-dimensional space in spherical coordinates. The estimated probability density function of (b) the fiber diameter; (c) the azimuthal angle φ; (d) the zenithal angle θ.

diameter, weighted by the inverse of its relative volume in the arithmetic mean calculation. It is given by

$$D_{iv} = \frac{1}{\sum_{i=1}^{N_f} \frac{1}{V_i}} \sum_{i=1}^{N_f} \frac{1}{V_i} D_i, \qquad (3)$$

When no weighting is applied, we also find the classical arithmetic mean called the mean diameter, and defined by $D_m = \sum D_i / N_f$.
Here, the microstructural descriptors of the medium are the porosity (ϕ); the anisotropy parameter (β), and the coefficient of variation (CV) [determined from the distributions of fiber diameters Fig.2b, angular orientation Fig.2d]. Their estimates for the studied cotton felt are given in Tab.1. Using these descriptors, we first obtain a periodic representation of the poly-disperse fibrous medium (PDFM); Fig. 3a. We then use Eq.2 and Eq.3 to calculate the volume-weighted mean diameter (D_v) and the inverse volume-weighted mean diameter (D_{iv}), respectively. These values are used to reconstruct the mono-polydisperse fibrous medium with volume-weighted mean diameter (MDFM-D_v,Fig. 3c) and with inverse volume-weighted mean diameter (MDMF-D_{iv},Fig. 3d). By increasing the size of the domain of the reconstructed samples, the mean value of the simulated porosity tends towards the experimental value. The standard deviation of the porosity with the sample of reconstructed fibrous media strongly decreases with the sample size. The RVE size was chosen to ensure that the ratio of the standard deviation over the mean value of the calculated porosity is less than $\epsilon = 0.1\%$.

$CV(\%)$	$D_m(\mu m)$	$D_v(\mu m)$	$D_{iv}(\mu m)$	β
40.3	13.5 ± 5.6	19.5 ± 0.3	8.9 ± 0.4	1.4

Table 1: Estimated microstructural descriptors of the cotton felt.

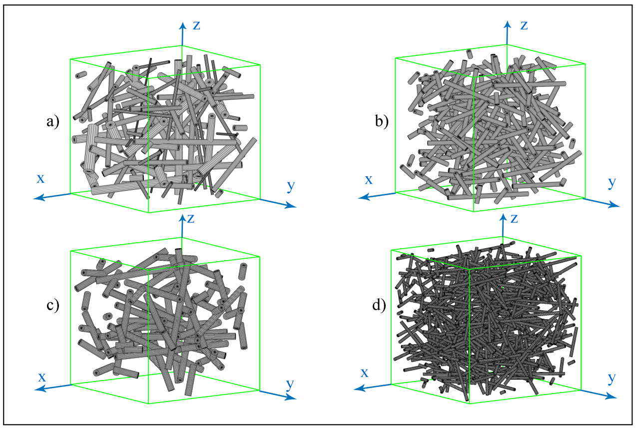

Figure 3: Randomly overlapping fiber periodic structures of cotton felt. (a) Polydisperse fibrous media (PDFM). (b) Monodisperse fibrous media (MDMF) with mean fiber diameter D_m. (c) Monodisperse fibrous media (MDMF) with volume-weighted mean diameter D_v. (d) Monodisperse fibrous media (MDMF) with inverse volume-weighted mean diameter D_{iv}.

3.2 Computation of transport parameters

The transport parameters under consideration comprise six parameters, namely ϕ, Λ', k_0, Λ, α_∞, and k'_0. They are calculated through numerical homogenization methods. The numerical homogenization methods provides input parameters to semi-phenomenological models to predict the acoustic properties (absorption and transmission coefficients) of the material. When computed from periodic unit cells such as the proposed RVEs, this creates a link between microstructural descriptors and macroscopic properties of acoustic materials.
A brief recall of the numerical homogenization methods is given in the next few lines. One solves different boundary value problems to retrieve the transport parameters.

For more details, the reader can refer to Ref. [6]. The low Reynolds number viscous flow equations (Stokes or creeping flow) are used to calculate the static viscous permeability k_0. The non-viscous flow or inertial equations are used to derive the high frequency tortuosity α_∞ and viscous characteristic length Λ. Additionally, the equation for thermal conduction is used to calculate the static thermal permeability k'_0. The open porosity ϕ and the thermal characteristic length Λ' are purely geometric parameters. They are directly calculated from the microstructure. In this work, all the boundary value problems were solved by the finite element method using Comsol Multiphysics software [17]. Two finite element meshes of the RVEs on which the boundary value problems are solved are shown in Fig.4. One is associated with The volume-weighted mean diameter D_v and the other with the diameter weighted by the inverse volume-weighted mean diameter D_{iv}.

The solutions for the velocity and temperature fields calculated on the previous two RVEs are shown in Fig.5. The determination of the low frequency asymptotic parameters (viscous static permeability k_0 and thermal static permeability k'_0) is based on the volume weighted mean diameter D_v in Fig.5a and Fig.5b. The high-frequency transport parameters (tortuosity α_∞, viscous characteristic length Λ, thermal characteristic length Λ') are estimated using the inverse-volume-weighted mean diameter D_{iv} in Fig.5c.

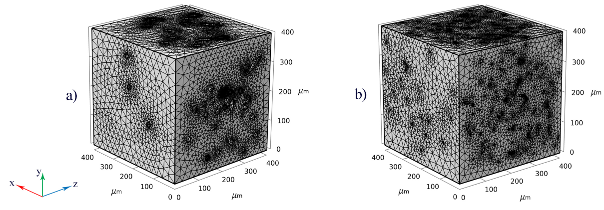

Figure 4: Typical mesh of cotton felt used to perform finite element (FE) simulations. a) Structure with the volume-weighted mean diameter with 811448 tetrahedral elements. b) Structure with the inverse volume-weighted mean diameter with 900380 tetrahedral elements.

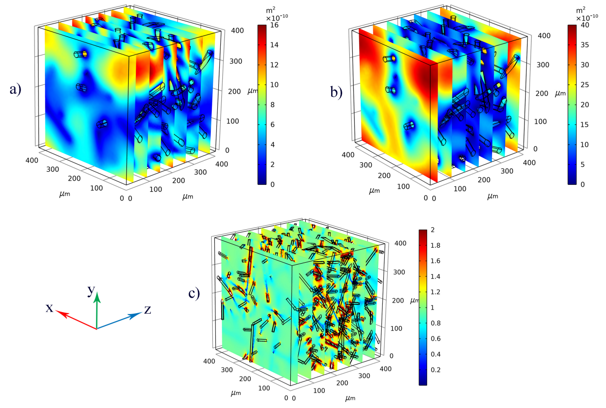

Figure 5: Asymptotic fields of velocity and temperature for the reconstructed RVEs of cotton felt: (a) velocity field expressed as local permeability (k_{0zz}) $[m^2]$ corresponding to Stokes flow in the z direction with RVE reconstructed by volume-weighted mean diameter. (b) Scaled heat diffusion field (k'_0) $[m^2]$ with RVE reconstructed by volume-weighted mean diameter. (c) Scaled velocity field corresponding to potential flow in the z direction $[-]$ with REV reconstructed by inverse volume-weighted mean diameter.

4. RESULTS AND DISCUSSION

The computed transport parameters for cotton felt fiber using a numerical approach are shown in Table 2. The first set of estimates are with the proposed two-RVE approach based on the D_v and D_{iv} weighted diameters, respectively. The second set of estimates are with a single RVE based only on the mean fiber diameter D_m. These estimates are compared to measurements of porosity (ϕ), resistivity (σ), and tortuosity (α_∞), as well as the estimated values of characteristic lengths (Λ, Λ') and thermal permeability (k'_0). It can be noted that the results of the two-RVE approach are in good agreement with the experimental data. This shows the role of polydiversity in the cotton felt studied and the need to take this polydiversity into account through the two RVE approach proposed. When the medium is highly polydisperse, the low-frequency microstructural descriptor is the volume-weighted mean diameter and the high-frequency microstructural descriptor is the inverse-volume-weighted mean diameter. This will be even more true when polydiversity is greater. Additional results on other felts will be presented at the conference to support this claim.

	ϕ	$\sigma(N.s.m^{-4})$	α_∞	$\Lambda(\mu m)$	$\Lambda'(\mu m)$	$k'_0(10^{-10}m^2)$
Single-RVE	0.948 ± 0.0002	67609 ± 1930	1.018 ± 0.001	67 ± 1	109 ± 1	4.99 ± 0.35
Two-RVE	0.948 ± 0.0004	33228 ± 3465	1.016 ± 0.003	49 ± 1	78 ± 1	9.4 ± 0.9
Measurements	0.948 ± 0.005	28684 ± 3664	1.023 ± 0.003	46 ± 3	74 ± 5	6.5 ± 0.8

Table 2: Macroscopic parameters: measurements and computational results of cotton Felt. Computation results are given for the proposed two-RVE approach and a classical single-RVE approach.

5. ACKNOWLEDGMENTS

This work was part of a project supported by ANRT and Adler Pelzer Group, Acoustic TechCenter R&D under convention CIFRE No.2020/0122. Partial support for this work was also provided by Université Paris-Est Sup (mobility grant from the ED SIE). The authors also acknowledge the support of the Natural Sciences and Engineering Research Council of Canada (NSERC) [funding with ref. number RGPIN-2018-06113]. We acknowledge Rémy Pires-Brazuna (ICMPE UMR 7189 CNRS) for SEM imaging of the fibrous samples.

6. REFERENCES

[1] V. Tarnow, "Airflow resistivity of models of fibrous acoustic materials," *The Journal of the Acoustical Society of America*, vol. 100, no. 6, pp. 3706–3713, 1996.

[2] Y. Xue, J. S. Bolton, R. Gerdes, S. Lee, and T. Herdtle, "Prediction of airflow resistivity of fibrous acoustical media having two fiber components and a distribution of fiber radii," *applied acoustics*, vol. 134, pp. 145–153, 2018.

[3] A. Tamayol and M. Bahrami, "Parallel flow through ordered fibers: an analytical approach," *Journal of Fluids Engineering*, vol. 132, no. 11, 2010.

[4] O. Umnova, D. Tsiklauri, and R. Venegas, "Effect of boundary slip on the acoustical properties of microfibrous materials," *The Journal of the Acoustical Society of America*, vol. 126, no. 4, pp. 1850–1861, 2009.

[5] F. Pompoli and P. Bonfiglio, "Definition of analytical models of non-acoustical parameters for randomly-assembled symmetric and asymmetric radii distribution in parallel fiber structures," *Applied Acoustics*, vol. 159, p. 107091, 2020.

[6] H. T. Luu, C. Perrot, V. Monchiet, and R. Panneton, "Three-dimensional reconstruction of a random fibrous medium: Geometry, transport, and sound absorbing properties," *The Journal of the Acoustical Society of America*, vol. 141, no. 6, pp. 4768–4780, 2017.

[7] H. T. Luu, C. Perrot, and R. Panneton, "Influence of porosity, fiber radius and fiber orientation on the transport and acoustic properties of random fiber structures," *ACTA Acustica united with Acustica*, vol. 103, no. 6, pp. 1050–1063, 2017.

[8] H. T. Luu, R. Panneton, and C. Perrot, "Effective fiber diameter for modeling the acoustic properties of polydisperse fiber networks," *The Journal of the Acoustical Society of America*, vol. 141, no. 2, pp. EL96–EL101, 2017.

[9] M. He, C. Perrot, J. Guilleminot, P. Leroy, and G. Jacqus, "Multiscale prediction of acoustic properties for glass wools: Computational study and experimental validation," *The Journal of the Acoustical Society of America*, vol. 143, no. 6, pp. 3283–3299, 2018.

[10] J. Schindelin, I. Arganda-Carreras, E. Frise, V. Kaynig, M. Longair, T. Pietzsch, S. Preibisch, C. Rueden, S. Saalfeld, B. Schmid, *et al.*, "Fiji: an open-source platform for biological-image analysis," *Nature methods*, vol. 9, no. 7, pp. 676–682, 2012.

[11] Y. Salissou and R. Panneton, "Pressure/mass method to measure open porosity of porous solids," *Journal of Applied Physics*, vol. 101, no. 12, p. 124913, 2007.

[12] J. F. Allard, B. Castagnede, M. Henry, and W. Lauriks, "Evaluation of tortuosity in acoustic porous materials saturated by air," *Review of scientific instruments*, vol. 65, no. 3, pp. 754–755, 1994.

[13] M. Henry, P. Lemarinier, J. F. Allard, J. L. Bonardet, and A. Gedeon, "Evaluation of the characteristic dimensions for porous sound-absorbing materials," *Journal of applied physics*, vol. 77, no. 1, pp. 17–20, 1995.

[14] R. Panneton and X. Olny, “Acoustical determination of the parameters governing viscous dissipation in porous media,” *The Journal of the Acoustical Society of America*, vol. 119, no. 4, pp. 2027–2040, 2006.

[15] K. Schladitz, S. Peters, D. Reinel-Bitzer, A. Wiegmann, and J. Ohser, “Design of acoustic trim based on geometric modeling and flow simulation for non-woven,” *Computational Materials Science*, vol. 38, no. 1, pp. 56–66, 2006.

[16] C. Peyrega, D. Jeulin, C. Delisée, and J. Malvestio, “3d morphological characterization of phonic insulation fibrous media,” *Advanced Engineering Materials*, vol. 13, no. 3, pp. 156–164, 2011.

[17] C. Multiphysics, “Introduction to comsol multiphysics®,” *COMSOL Multiphysics, Burlington, MA, accessed Feb*, vol. 9, p. 2018, 1998.